



## Optimal foraging by zooplankton within patches: The case of *Daphnia*

Ricardo Garcia <sup>a</sup>, Frank Moss <sup>a,\*</sup>, Ai Nihongi <sup>b</sup>, J. Rudi Strickler <sup>b</sup>,  
Sebastian Göller <sup>c</sup>, Udo Erdmann <sup>c</sup>, Lutz Schimansky-Geier <sup>c</sup>, Igor M. Sokolov <sup>c</sup>

<sup>a</sup> Center for Neurodynamics, University of Missouri at St. Louis, St. Louis, MO 63121, USA

<sup>b</sup> Great Lakes WATER Institute, University of Wisconsin at Milwaukee, Milwaukee, WI 53204, USA

<sup>c</sup> Laboratory for Applied Stochastic Processes, Institute of Physics, Humboldt University of Berlin, D-12489 Berlin, Germany

Received 22 May 2006; accepted 28 November 2006

Available online 12 February 2007

---

### Abstract

The motions of many physical particles as well as living creatures are mediated by random influences or ‘noise’. One might expect that over evolutionary time scales internal random processes found in living systems display characteristics that maximize fitness. Here we focus on animal random search strategies [G.M. Viswanathan, S.V. Buldyrev, S. Havlin, M.G.E. Da Luz, E.P. Raposo, H.E. Stanley, Optimizing the success of random searches, *Nature* 401 (1999) 911–914; F. Bartumeus, J. Catalan, U.L. Fulco, M.L. Lyra, G.M. Viswanathan, Optimizing the encounter rate in biological interactions: Lévy versus Brownian strategies, *Phys. Rev. Lett.* 88 (2002) 097901 and 89 (2002) 109902], and we describe experiments with the following *Daphnia* species: *D. magna*, *D. galeata*, *D. lumholtzi*, *D. pulicaria*, and *D. pulex*. We observe that the animals, while foraging for food, choose turning angles from distributions that can be described by exponential functions with a range of widths. This observation leads us to speculate and test the notion that this characteristic distribution of turning angles evolved in order to enhance survival. In the case of theoretical agents, some form of randomness is often introduced into search algorithms, especially when information regarding the sought object(s) is incomplete or even misleading. In the case of living animals, many studies have focused on search strategies that involve randomness [H.C. Berg, *Random Walks in Biology*, Princeton University, Princeton, New Jersey, 1993; A. Okubo, S.A. Levin (Eds.), *Diffusion and Ecological*

---

\* Corresponding author. Tel.: +1 314 516 6150; fax: +1 314 516 6152.

E-mail address: [mossf@umsl.edu](mailto:mossf@umsl.edu) (F. Moss).

Problems: Modern Perspectives, second ed., Springer, New York, 2001]. A simple theory based on stochastic differential equations of the motion backed up by a simulation shows that the collection of material (information, energy, food, supplies, etc.) by an agent executing Brownian-type hopping motions is optimized while foraging for a finite time in a supply patch of limited spatial size if the agent chooses turning angles taken from an exponential distribution with a specific stochastic intensity or ‘noise width’. Search strategies that lead to optimization is a topic of high current interest across many disciplines [D. Wolpert, W. MacReady, No free lunch theorems for optimization, *IEEE Transactions on Evolutionary Computation* 1 (1997) 67].

© 2007 Elsevier Inc. All rights reserved.

*Keywords:* Zooplankton; Optimal foraging; Natural selection; Natural stochastic resonance

---

## 1. Introduction

The spatial diffusion of aggregations of various animals has received a great deal of interest for many years [1–3]. Observations of living organisms in the process spreading from a point of aggregation or artificial release have led to the development of physical diffusion theories applied to these and similar processes [3,4,6–10]. All animal motions involve randomness, or noise, to some degree [9,11]. This has led to two general theoretical approaches for modeling animal motions: methods based on random walk theory, of which there are many, but we cite here only one [3], and those based on continuous stochastic differential equations [10,12,13]. An essential activity for any animal, and the process that we focus on here, is foraging for food [14–22], specifically, foraging in food patches of finite size [23–28]. We consider foraging in a food patch of determined size, over which there is a uniform food distribution. Additionally, we add the constraint that foraging can continue only for a finite time.

Optimization problems [5] have attracted the attention of a number of groups [1,22,30,31]. The optimum foraging strategy depends strongly on the density of food particles, or prey, in the patch in comparison with the typical length of a characteristic movement of the animal. If food density is small, it has been shown that a search strategy based on Lévy rather than Brownian statistics is optimal [1,2]. Other approaches have included fractal analyses of swimming motions [18,32–34]. In the below described experiment, theory and simulations, the food density was high, and we therefore confine our analyses to consideration of Brownian-type statistics.

We concentrate on the motions of single individuals while feeding. *Daphnia* are not social animals. Solitary individuals are observed to swim alone with no apparent distress. In order to define the simplest possible yet feasible problem, we study the swimming characteristics that arise only from the stimuli offered by the presence of uniformly distributed food. It is important, therefore, to eliminate insofar as possible all other stimuli, for example those arising from light, from neighboring individuals or from the walls or bottom of the aquarium. The experiments described below were carried out in the absence of visible light. A solution containing a uniform distribution of food was used in order to eliminate stimuli that would arise from patchiness or non-uniform distributions. In order to minimize animal–animal interactions, the density was kept low enough that approximately 1 cm separated nearest neighbors. Individuals swimming near the walls or bottom of the container were not considered. The theory described below was developed to describe this

type of motion, thus no interaction terms appear in it. These considerations stand in contrast to the many works that describe swarming and pattern formation in colonies of various types of animals wherein the interactions among individuals is crucially important, see for example Refs. [4,15,23].

The motion we consider in two dimensions is a sequence of straight line hops, each followed by a pause, then a change of direction through a *turning angle*  $\alpha$ , followed by another hop, etc. Our initial application is to the swimming characteristics of various species of the zooplankter, *Daphnia*, while foraging for food. We observe, in both theory and the simulations described below, that the quantity of food collected is optimized with a statistical parameter associated with the stochastic intensity, or the magnitude of the variability, of the turning angles chosen by the animal as it moves within the patch. The maximization of a desirable quantity, here the amount of food gathered, at an optimal value of the stochastic, or noise, intensity recalls the process of *stochastic resonance*, which we discuss further in Section 8.

We emphasize the importance of the statistical *distribution* of the observed turning angles. The width of this distribution, here called the ‘noise width’, is a measure of the stochastic intensity of the underlying random process. A number of authors have reported tabulations of or the average of turning angles during observations or analyses of animal motions [17,18,29,34,35] while others [1,12,29,44,45] have included the distribution function of this quantity. We discuss these in more detail in Section 8.

The hop–pause–turn–hop motion reminds one of a physical random walk, and indeed such ideas have been applied to numerous living creatures ranging in size from bacteria to birds and large mammals [3,4]. Foraging, of course, is an essential activity for all animals that involves searching areas that might contain food, eating when it is found and then moving on. The process is semi-random in that instantaneous and local decisions made by the animal depend to some extent not only on chance but also on some immediate objective knowledge that hopefully maximizes success. Thus the foraging animal can be expected to diffuse (in our case over a two dimensional plane), and its motion can be described as a correlated random walk (CRW). Such diffusion has been well studied across a wide spectrum of living creatures [3,4,6,9,17,38–42].

But here we focus on optimization of the diffusion process, specifically in order to maximize success for random encounters with food particles in finite spatiotemporal scales. We ask what characteristics of the essentially random search process can lead to enhanced foraging success. We have observed that our foraging *Daphnia*, of the species studied here, do not mimic purely Brownian motion, wherein each move has no correlation with any previous move but instead choose from specific distributions of motional parameters. Previous studies have revealed some of the characteristics of the combination of random and deterministic motions of plankton [9,32,46]. Here we consider the *turning angle*,  $\alpha$ . This leads us to formulate the following hypothesis: The *distribution* of turning angles in the hop–pause–turn–hop sequence is selected for survival. Success at foraging for food, as well as other behaviors, that enhance fitness, have been the subject of many studies, of which we cite only a few [31,47,48]. Support for the hypothesis would be generated if one could show that the observed turning angle distributions (TADs) lead to a maximization of food gathering.

As we show below, the observed TADs of our foraging *Daphnia* are well described by exponential functions:  $P(\alpha) = N_0 \exp[-|\alpha|/\sigma_0]$ , where  $N_0$  is the number of angles observed,  $|\alpha|$  is the magnitude of the turning angle, and  $\sigma_0$  is the width of the distribution, here called the ‘noise width’.

We note that such distributions lie between two extremes: In the limit of large  $\sigma_0$ ,  $P(\alpha) \rightarrow const$ , while at the opposite extreme, for  $\sigma_0 \rightarrow 0$ ,  $P(\alpha) \rightarrow \delta(\alpha_0)$ . In the first limit, the animal or agent executes purely uncorrelated Brownian motion, while in the latter limit the animal does not turn at all but follows straight line or ballistic motion as shown in Fig. 1. (Throughout this paper, we use the word ‘animal’ or ‘Daphnia’ when referring to the experimental observations of the actual *Daphnids*, while ‘agent’ is used in reference to the theoretical or simulated creature. ‘Particle’ refers to representation of the food particles in the theory or simulation.)

The first order correlation function,  $\Omega = \int_{-\pi}^{\pi} P(\alpha) \cos(\alpha) d\alpha$ , is a quantitative measure of the differences among distributions such as those indicated in Fig. 1 and as discussed in Sections 5 and 6. The original theory is based on continuous stochastic differential equations [12], but a CRW version which connects to the extensive literature on this topic has also been developed [49].

We discuss some characteristics of *Daphnia* that are relevant to our study in Section 2. In Section 3, we present the methods used for *Daphnia* culture, in the experiment, for data analysis and in the simulations. We present the results of the experiment in Section 4 for five species including two morphological forms of one and for both adults and juveniles of two species. In Section 5, we summarize and present the results of the theoretical model based on stochastic differential equations. Section 6 shows two versions of a simulation based on CRWs with the simplest possible assumptions regarding the collection of material by random walkers who choose turning angles from correlated TADs. In Section 7, we examine again the hypothesis in the light of the experimental results and make some remarks on the diffusion process. In Section 8, we summarize and discuss our results in relation to other relevant studies as reported in the literature. Finally, we associate the maximum in food gathered at an optimal value of the noise width of the TAD, as predicted both by the theory and by the two simulations, to a new kind of stochastic resonance arising from randomness in the animal’s own internal systems.

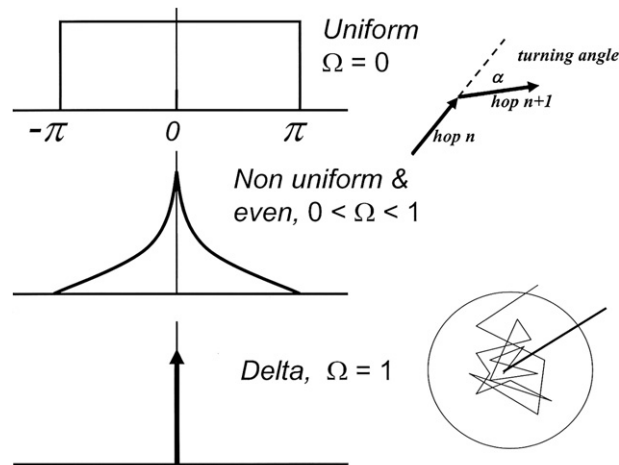


Fig. 1. Possible turning angle distributions showing the extremes: uncorrelated (top) and delta-function, or no turns (bottom). The exponential TAD lies in between these extremes. Insets: (top) two hops that define the turning angle,  $\alpha$ , (bottom) hop trajectories showing a non-uniform distribution (the zig-zag trace) and delta-correlated no turns (the dark straight line).

## 2. Some characteristics of *Daphnia* species

*Daphnia* normally feed during nighttime darkness on photosynthetic algae which they find near the water surface and which were produced during the previous day. During the daylight hours they descend to the bottom of the lake or pond. This behavior is called diel vertical migration [50,51] and is thought by most biologists to have evolved in order to escape predators [50,52,53] such as fish that hunt them visually. Three-dimensional tracking of *Daphnia* indicate that they normally swim in approximately two-dimensional planes ( $\pm 2$  cm) [33]. *Daphnia* are attracted to visible light [54], flee from ultra violet [55] and are widely assumed to be blind to infra red.

## 3. Methods

### 3.1. Culture

The animals used in the experiments described here were cultured in five species in two different labs. *D. glaeata*, *D. lumholtzi* (in two morphotypes: with and without helmets or spines), *D. pulex*, and *D. pulex* adults were cultured in Milwaukee at the Great Lakes WATER Institute. Typically 20–30 individuals of each species were kept in 1-l of well water at approximately 21 °C with 24 h of light. Two 32 W fluorescent lights were located approximately 30 cm distant from the five cultures. The animals in Milwaukee were fed with a mixture of three live phytoplankton species (with UTEX culture number): *Ankistrodesmus falcatus* (UTEX 101), *Chlamydomonas reinhardtii* (UTEX 90), *Selenastrum capricornutum* (UTEX 1648) and maintained in well water under fluorescent light at concentrations in the range  $(7.2\text{--}14.2) \times 10^4$  cells/ml such as to make the water pale green. Laboratory air was bubbled through the mixed phytoplankton culture at the rate of about 5 bubbles per second (2 mm bubbles). About 10 ml of this phytoplankton mixture was added to each *Daphnia* culture daily. New water was added to the *Daphnia* cultures daily to make up for water loss due to evaporation. Excess adult individuals were removed from the culture daily in order to maintain a population within the 1-l beakers of approximately 20–30 individuals. The water was exchanged completely approximately once each month. All equipment, tools and containers used for culturing both *Daphnia* and the phytoplankton were autoclaved before use in order to avoid contamination with bacteria.

The *D. pulex* and *D. magna*, both adults and juveniles, were cultured in St. Louis at the Center for Neurodynamics. These two species differ considerably, *D. pulex* being more gracile, though their anatomical features are much the same. Typical features of a pair of adult individuals are shown in Fig. 2.

*D. pulex* were hatched from their resting eggs (Carolina Biological) in well water in a Petri dish. Often predators appear as well. In order to obtain a pure *Daphnia* culture, individuals were extracted from the dish with a suction pipette and examined in a single drop of water under a microscope. If the individual within the droplet was free of other living organisms (at least those visible under the microscope), it was added to a culture medium consisting of 1-l of well water plus a few milligrams of *Daphnia* food (Carolina Biological) consisting of a mixture of unknown species of photosynthetic phytoplankton. The selection process was repeated until 20–30 individuals were in the culture medium. The culture was maintained perpetually under a fluorescent light (14 W bulb)

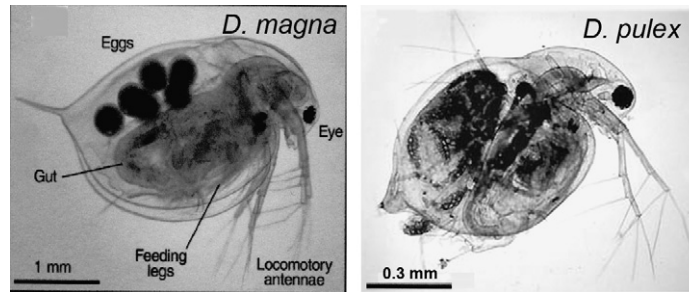


Fig. 2. Examples of adult *D. magna* and *D. pulex*.

70 cm above the beaker. The phytoplankton growing within the culture, and upon which the *D. pulex* feed, were fed twice weekly with 10 ml of a dilute solution of micro-fine size freeze dried algae, *Spirolina patensis* (Algae-Feast, Earthrise Nutritionals). This solution was made by dissolving approximately 55 mg of *Spirolina* in 1-l of well water. About 50% of the culture water was replaced with clean well water weekly. Under these conditions the *D. pulex* population increases rapidly. After a few days the population was moved to a larger 3 liter beaker and the feeding routine continued. In order to avoid overcrowding it was necessary to remove about half the population every 2 weeks.

The *D. magna* were obtained from a permanent culture maintained by the Biology Department at University of Missouri at St. Louis. They were maintained in two large (45 and 25 l) aquaria placed in front of a window and maintained at laboratory room temperature (21–23 °C). The aquaria received some natural daylight from the window and perpetual fluorescent light from a 14 W bulb placed 70 cm above the aquaria and midway between them. They were fed twice weekly with about 40 mg (large aquarium) and 20 mg (small aquarium) of the aforementioned freeze dried *Spirolina* dissolved in well water. This solution was sufficient to make the aquarium water noticeably green. About 50% of the aquarium water was replaced with clean well water weekly (before feeding). About 25% of the *D. magna* individuals were discarded with the weekly water change in order to keep the population density of adults in bounds at approximately 500 per liter. Under these conditions, the population fluctuates on an approximately monthly time scale. The *D. magna* usually formed a noticeable swarm shaped approximately like a 14 cm diameter sphere, under the fluorescent light or near a reflection of it from the bottom wall of the aquarium. During times of maximum population and good health (as evidenced by the presence of relatively large numbers of juveniles) we measured the density of individuals within the swarm. This was done by rapidly extracting about 40 ml with a large suction pipette (actually a turkey baster) from the center of the swarm. The results were approximately 1 adult and 2.4 juveniles per 2 ml. These results may, however, be biased on the low side, since *Daphnia* exhibit an induced escape reflex when they perceive a water flow such as near the entrance of the pipette. Moreover, the escape success of juveniles and adults may be different.

Both culture methods, though quite different, work very well and are well known and widely used by various groups working with *Daphnia*. The St. Louis method is suitable for producing large populations, for example, as needed for experiments with swarms. The Milwaukee method is suitable for culturing small populations of many different species in limited lab space.

Table 1  
*Daphnia* Species turning angle distribution width,  $\sigma_0$

Species: <i>D.</i>	Lab	$\sigma_0$ (rad)	$\sigma_0$ (deg)	TAD
<i>pulex</i> – adult	Mil	$0.82 \pm 0.1$	$47.0 \pm 5.7$	Fig. 7
<i>pulex</i> – adult	StL	$0.74 \pm 0.1$	$42.4 \pm 5.7$	Fig. 6
<i>pulex</i> – juvenile	StL	$0.52 \pm 0.05$	$29.7 \pm 2.9$	Fig. 7
<i>magna</i> – adult	StL	$1.2 \pm 0.1$	$68.8 \pm 5.7$	Fig. 6
<i>magna</i> – juvenile	StL	$1.0 \pm 0.2$	$57.3 \pm 11.5$	Fig. 7
<i>galeata</i>	Mil	Non exponential TAD		
<i>lumholtzi</i> – spine	Mil	$2.3 \pm 0.4$	$131.8 \pm 22.9$	Fig. 7
<i>lumholtzi</i> – no spine	Mil	$1.0 \pm 0.1$	$57.3 \pm 5.7$	Fig. 7
<i>pulicaria</i>	Mil	$0.92 \pm 0.06$	$52.7 \pm 3.4$	Fig. 7

The ultimate test of any culture method is the health of the populations. In the case of *Daphnia*, good health is assured so long as juveniles are present in significant numbers in the populations. In both labs, individuals were chosen for the experiments only from the cultures when large numbers of juveniles were present. However, in order to test the reproducibility of the results, experiments with *D. pulex* adults were carried out in both labs. As shown above in Table 1, the results for this species were reproducible across the two labs within the statistical precision of the measurements.

### 3.2. Experimental procedure and apparatus

Video records of the swimming motions of *D. magna* and *D. pulex*, adults and juveniles, were made in St. Louis using the apparatus shown in Fig. 3.

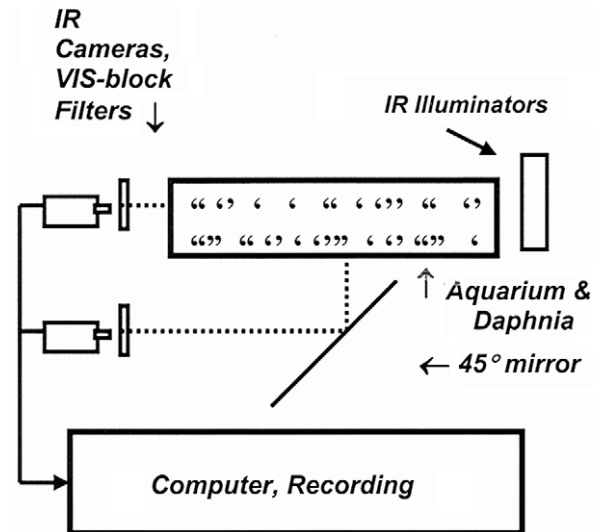


Fig. 3. The apparatus. Cameras view both side and bottom views of swimming *Daphnia* in a shallow aquarium (~2 cm water depth) in the infra red. The experiments were performed in nearly complete absence of visible light. The Milwaukee apparatus differed in that IR illumination was from the bottom through a diffuser instead of the 45° mirror, and a single camera was located above the aquarium.

The remaining species were recorded in Milwaukee using a similar apparatus. Typically about 8–12 individuals were placed in a standard feeding solution 1.5–2 cm deep in a shallow square transparent aquarium,  $26 \times 26 \times 5$  cm constructed of Perspex, which is transparent to both visible and infra red light in the wavelength ranges used. The standard feeding solution for making the video records differed from the feeding solution used for culturing in two respects: first, the concentration of food or prey cells was much smaller than in the culturing medium, and second, the solution was well mixed, so that the prey distribution was uniform. In Milwaukee, the standard feeding solution for making video records was  $3.0 \pm 0.6 \times 10^3$  cells/ml well water of live *C. reinhardtii*. In St. Louis, the standard feeding solution for video records was  $8 \pm 1.6 \times 10^3$  cells/ml (equivalent to 13.7 mg/l) freeze dried *Spirolina*. In both cases the cell counts were accomplished with a bright line counting chamber (Hausser Scientific, Horsham, PA). In both, feeding solutions used in filming the prey (food) density was intended to be small enough that it would not show up significantly under the infra red light used for making the video records, but large enough that many (approximately 100) prey encounters would occur during one hop-pause episode. During the actual experiment and recording of videos, the density of individual animals was much smaller than that shown in the example frame Fig. 4. During recording, typically 1–2 cm separated individuals in order to minimize individual–individual interactions.

The *Daphnia* (typically 8–12) to be used in the experiments were extracted from the cultures and placed in the aforementioned square aquarium containing the standard feeding solution for video recording. Before recording *D. pulex* and *D. magna*, both adults and juveniles were maintained in the dark for 15–30 min. Before recording, all visible light was extinguished, and the infra red (IR) illuminators (American Dynamics 1020) and the digital cameras were switched on. The recording cameras were Sony DCR-TRV80 (St. Louis) and XC-ES50CE (Milwaukee) operating at 30 frames per second. This frame rate established the time base of the recordings. Both cameras can record in the wavelength range available from the illuminators ( $>730$  nm). The digital video recordings were 8–12 min long and were captured directly by computer. Fig. 4 shows a single frame from such a video of *D. magna* (though for illustrative purposes, the density of animals is much larger than in the actual experiments).

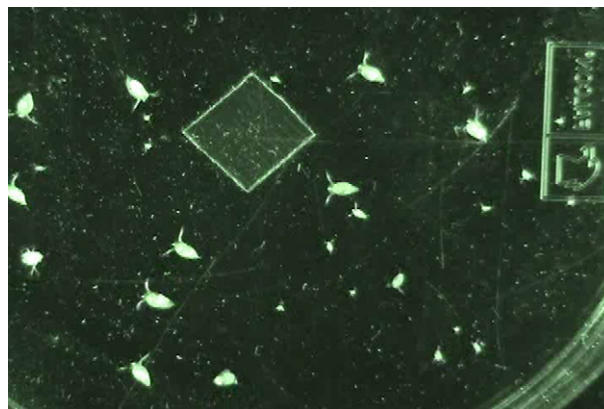


Fig. 4. An example frame from the video records showing *D. magna* adults and juveniles. The square is a 1 cm distance calibrator. In the actual recordings, many fewer individuals were used in order to minimize effects of animal–animal interactions.

Three ages of *D. magna* are shown in Fig. 4. The largest individuals are adults that are reproducing. The intermediate size individuals are no older than about 24 h, and the smallest are about 8–12 h old. For the experiments with juveniles, about 3–5 adults were placed in the standard feeding solution and allowed to remain in the dark for about 12 h. Then the adults were then removed, the feeding solution renewed, and videos of the juveniles were made again after about 30 min conditioning in the dark.

### 3.3. Data analysis

The object in the center of Fig. 4 is a 1 cm square calibrator. The coordinates (in pixels) of each corner of this square were obtained and the scalar distance between adjacent corners calculated using the Pythagorean Theorem. In this way the conversion factor relating lengths in pixels to those in cm was obtained. Thus from the sequence of coordinates at the beginnings and ends of the hop vectors, and using the conversion factor, the hop lengths could be obtained, again using the Pythagorean Theorem. For statistical accuracy typically 750 or more hops were analyzed usually from 4 to 6 different animals. Only animals swimming far ( $>1\text{--}2$  cm) from the aquarium walls were analyzed. We also tabulated hop length, hop time, and pause time as will be analyzed and reported in detail elsewhere.

After the video records were obtained, the movies were reviewed in order to identify the frames containing the beginning and end of a hop. These frames were exported and a software program, *Track-It* (Iguana Gurus, <thegurus@ameritech.net>), was used to locate and record the  $x$ - $y$  coordinates (in pixels) of an identifiable point on the animal's body. The identifiable point was usually the head midway between antennae. We observed that while feeding under the aforementioned conditions, the animals rarely tumbled or turned during a single hop. In the few cases where this did happen (see the individual about 1/3 of the way up on the extreme left of Fig. 4) that hop was not included in the analysis. In all cases considered the individual was pointed in the vector direction of the hop both at the beginning and at the end of the hop. Thus we have the coordinates in pixels at the beginning,  $x_1, y_1$ , and at the end,  $x_2, y_2$ , of each hop in a sequence. These coordinates define the beginning and end points of the first hop vector as shown in the inset of Fig. 1. The second hop vector is obtained by repeating this procedure on a second pair of exported frames that define the beginning and end of the second hop and so on. The tracking program writes all the coordinates sequentially in tabular form to an Excel file. A simple program then constructed beginning-to-end hop vectors and computed the angles between sequential vectors. This was done by first locating the quadrant where was located the tip of each vector. The angle  $\phi_i$  with respect to the positive  $x$ -axis was calculated from  $\phi_i = \tan^{-1}[(y_2 - y_1)/(x_2 - x_1)]$ , for the  $i$ th hop. The turning angle was obtained from these angles,  $\alpha_i = \phi_{i+1} - \phi_i$ . Positive turning angles represent right turns and negative ones turns to the left. No turning angle greater than  $180^\circ$  was included, though such events are so rare that usually not one occurred in a sample of hundreds of angles. Note that the tip of one vector need not join to the tail of the next one. From the tabulations of the turning angles, frequency histograms were then obtained as shown by the examples in Fig. 5.

Fig. 5 shows two turning angle frequency histograms, also here called TADs (turning angle distributions), as obtained using the aforementioned procedure. We note that the TADs are approximately symmetric in positive (right turn) and negative (left turn) angles. The symmetry of these

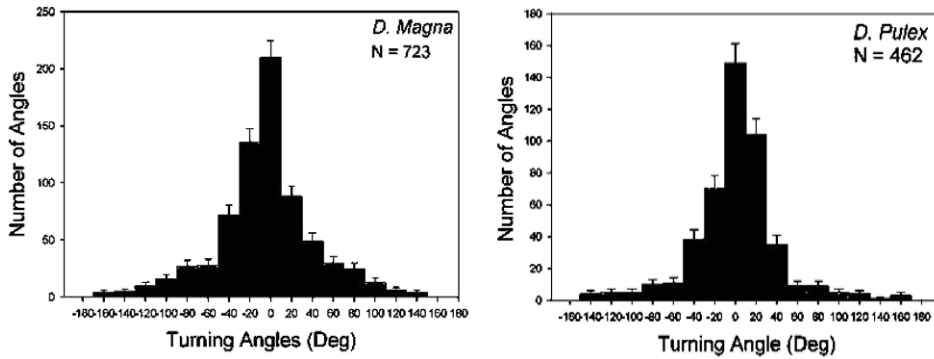


Fig. 5. Turning angle frequency histograms for *D. magna* (left) and *D. pulex* (right) adults.

TADs indicates that during the experiment there were no significant stimuli that induce motions in a specific direction as would occur if extraneous significant stimuli were present, for example as presented by a patchy or non-uniform distribution of prey or by stray visible light. Another example of motion wherein asymmetric TADs are observed is the rotational motion [12,13] induced by the presence of light sources visible to large populations (colonies) of the animals [56,57]. Since *Daphnia* respond to visible light, in order to avoid asymmetric TADs, care was taken to perform the experiments in darkness (ambient visible light intensity smaller than 2.5 nW/cm<sup>2</sup>).

These data were analyzed by plotting frequency histograms of the *magnitudes* of the angles on semi-logarithmic axes. The aforementioned exponential behaviors thus show as straight lines on such a plot with slopes  $1/\sigma_0$ . As examples, including the linear analyses, the data of Fig. 5 are re plotted on semi-logarithmic scales in Fig. 6. Both distributions can be described by exponential functions as mentioned previously. This becomes evident once the TADs are plotted as absolute (unsigned) angles on semi-logarithmic scales as allowed only if the TADs of the signed angles are symmetric. Examples together with the straight lines representing the fitted exponential functions are shown in Fig. 6.

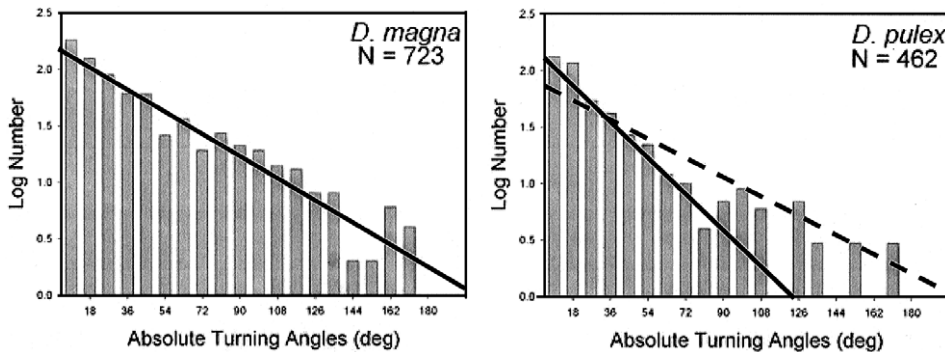


Fig. 6. The same data as shown in Fig. 5 but the frequencies of the unsigned angles are plotted on semi-logarithmic scales. The straight lines are fits to the exponential function,  $P(x) = N_0 \exp\left[-\frac{|x|}{\sigma_0}\right]$  with noise widths  $\sigma_0 = 1.2 \pm 0.1$  (*magna*) and  $0.74 \pm 0.1$  (*pulex*—dashed) and 2.18 rad (*pulex*—solid) obtained by least squares fits to the TADs. The dashed fit was used in the analysis. These data were obtained in St. Louis.

Note that in the case of *D. pulex* there is a departure from exponential behavior at large angles. Such departures were evident in a very few cases of the other data as well, and may represent a transition to a non-exponential behavior at large angles. A fit taking this into account is shown by the solid line in the right panel of Fig. 6. The dashed line in the same panel ignores the large angle anomaly. In order to avoid subjective judgments that might be prompted by trying to guess the angle above which the behavior becomes non-exponential, we analyzed all data by linear least squares fits on the full interval  $0-\pi$  as shown by the dashed line. The statistical precision of the fits is indicated by the standard errors as shown in the caption of Fig. 6. Data for all five adult species plus the juveniles of *D. magna* and *D. pulex* and the two morphological forms of *D. lumholtzi* were analyzed following exactly the same procedure as the examples shown in Fig. 6.

#### 4. Experimental results

An exponential function, with  $\sigma_0$  as a fitting parameter, was fit to each set of data shown in Fig. 7 by linear regression, exactly as was done for the St. Louis data shown in Fig. 6. The results of least square fits to exponential functions for all species both juveniles and adults, and for the two morphological forms, are shown in Table 1, Section 3.1. We note that the noise widths of the TADs vary from a minimum of  $29.7^\circ$  (*D. pulex* juvenile) to a maximum of  $131.8^\circ$  (*D. lumholtzi* with spines) with an average for the eight sets of  $1.06$  rad or  $60.7^\circ$ .

Table 1 tabulates the experimentally determined fitting parameter  $\sigma_0$  for all species as shown in the third and fourth columns. The species are identified in the first column. The lab where the specific experiment was carried out is shown in the second column. The Figure where the TAD is displayed is tabulated in the fifth column. Animals whose age status is not specified are adults.

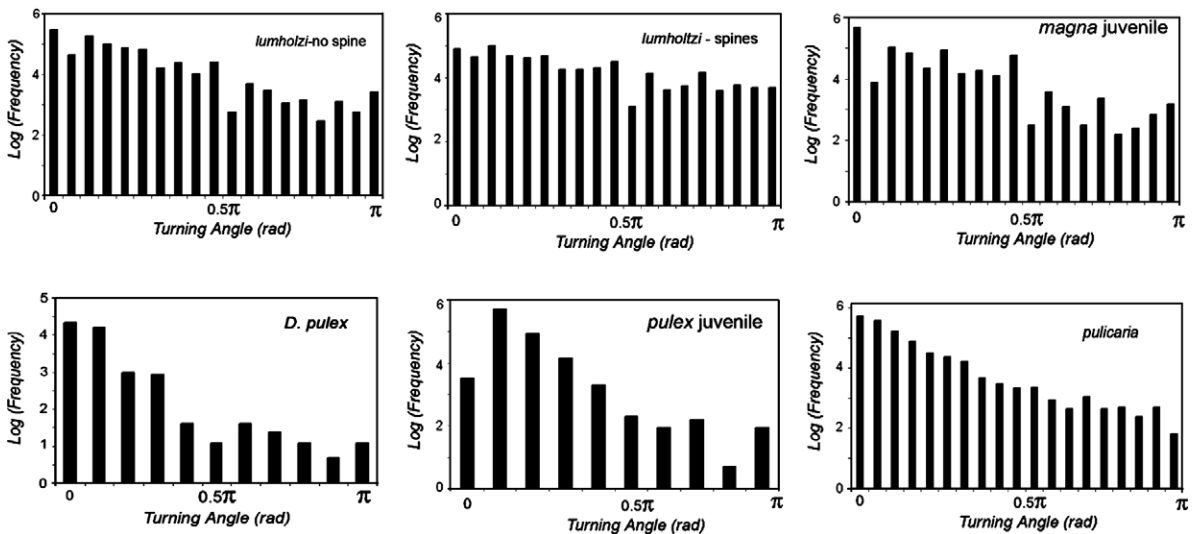


Fig. 7. Histograms of the turning angles for all species except *D. magna* adult and physical forms plotted on logarithmic scales. Note that this Figure includes a second set for *pulex* adults obtained in Milwaukee, which serves as a control of consistency between the two labs. Exponential functions (not shown) would appear as straight lines which are better representations of some data than others, for example *D. pulicaria*.

Of these, the first two entries in [Table 1](#), the results of experiments with *D. pulex* adult, were repeated in both labs with different animals cultured in the lab specified. The results can be compared:  $0.74 \pm 0.1$  rad (St. Louis) and  $0.82 \pm 0.1$  rad (Milwaukee). These differ by 11% which may be considered an estimate of the minimum overall reproducibility or accuracy of the experiments. However, since this difference falls within the limits of statistical precision of the two results ( $\pm 0.1$  rad), it may be considered a test of the reproducibility of experiments carried out in Milwaukee versus those carried out in St. Louis.

We obtained data also on the hop lengths, hop times and pause times. We here report only the means of those three quantities and only for *D. magna* adult as obtained in St. Louis. In every case more than 750 hops were analyzed to arrive at the mean and its standard deviation. The mean hop length is  $\langle \ell \rangle = 1.11 \text{ mm} \pm 0.02 \text{ mm}$ . The mean hop time is  $\langle t_h \rangle = 0.15 \pm 0.033 \text{ s}$ , and the mean pause time is  $\langle t_p \rangle = 0.25 \pm 0.033 \text{ s}$ . The errors for the two times are actually the limits of precision of the cameras operating at 30 frames/s.

## 5. Theory of optimal foraging

We have developed a foraging theory, based on continuous stochastic differential equations of motion for an individual agent (animal), as described below. The simulations of foraging agents described in the next section are in qualitative agreement with the theory.

In a previous work [12] a CRW model was applied to find the effective diffusion coefficient of the random motion with preferred turning angles. Starting with the spatial correlation function of such a random walker, and using the approach of Kareiva and Shigesada [58–61], we derived the diffusion coefficient as a function of the angular correlation function. The angular correlation depends on the ensemble of turning angles chosen by the agent while foraging in a food patch. Knowing the TAD, the diffusion coefficient can easily be calculated. It was shown that with a preferred turning angle of, say  $30^\circ$ , the agent could cover a larger area in the mean than an agent executing a pure Brownian (uncorrelated) motion. Here we first summarize the theory presented in Ref. [12], where a simple approach leads to the diffusion coefficient of a persistent random walker. After comparison with some of the experimental results presented above, we present a simple theory of food consumption.

### 5.1. Effective diffusion of a persistent random walk

To calculate the effective diffusion of a random walker, or agent, Kareiva and Shigesada [59,61,62] found that it is sufficient to record the angular correlation of the aforementioned walk. The relative angle between successive hop directions is crucial. Using this idea Komin et al. [49] calculated the diffusion coefficient of a CRW depending on this correlation. The result is the effective diffusion constant in a two-dimensional space:

$$D_r \approx \frac{\lambda^2}{4\tau} \frac{1 + \Omega}{1 - \Omega}, \quad (1)$$

where  $\lambda$  is the mean hop-length,  $\tau$  is the mean hop time of the agent, and  $\Omega$  is the angular correlation between two successive hops with turning angle  $\alpha$ . As mentioned above,

$$\Omega = \int_{-\pi}^{\pi} P(\alpha) \cos \alpha \, d\alpha. \tag{2}$$

From the experiments we observe that the TADs are well described by the exponential function,

$$P(\alpha) = C \exp\left(-\frac{|\alpha|}{\sigma_0}\right). \tag{3a}$$

When properly normalized, the constant is

$$C^{-1} = \int \exp\left(-\frac{|\alpha|}{\sigma_0}\right) \, d\alpha = \frac{1}{2\sigma_0\left(1 - \exp\left(-\frac{\pi}{\sigma_0}\right)\right)}, \tag{3b}$$

where we note that  $2\sigma_0$  is the double width of the TAD. Inserting Eq. (3) into Eq. (2), one obtains the angular correlation,

$$\Omega = \left(\frac{1}{\sigma_0^2 + 1}\right) \frac{1 + \exp\left(-\frac{\pi}{\sigma_0}\right)}{1 - \exp\left(-\frac{\pi}{\sigma_0}\right)}. \tag{4}$$

This is a function which decays with the width  $\sigma_0$  of the exponential distribution.

### 5.2. Theory of food consumption

Let us now speculate on the advantages of motion for which the diffusive behavior has been chosen by these animals in between the uncorrelated Brownian and the straight line ballistic flight. Consider the following model of a foraging agent which we represent as a diffusing entity. A group of such agents can be described by a continuous density  $\rho(\vec{r}, t)$  which obeys a diffusion equation with the coefficient  $D_r$  from Eq. (1),

$$\frac{\partial \rho}{\partial t} = D_r \Delta \rho. \tag{5}$$

In two-dimensions the resulting probability density is

$$\rho(\vec{r}, t) = \frac{1}{4\pi D_r t} \exp\left(-\frac{\vec{r}^2}{4D_r t}\right). \tag{6}$$

We assume that a single agent consumes food at a constant rate  $k$ , the clearance rate in two-dimensions, during its random motion, and that the density of food particles is given by  $c(\vec{r}, t)$ . In addition, the food is assumed to be approximately immobile, that is, it diffuses very slowly in comparison with the agent. The food density is thus given by

$$\frac{\partial}{\partial t} c(\vec{r}, t) = -kc(\vec{r}, t)\rho(\vec{r}, t), \tag{7}$$

which can easily be solved using the known agent density, Eq. (6). Simple quadrature gives

$$c(\vec{r}, t) = c_0(\vec{r}) \exp\left[-\int_{t_0}^t k\rho(\vec{r}, t') \, dt'\right], \tag{8}$$

so that

$$c(\vec{r}, t) = c_0(\vec{r}) \exp \left[ -\frac{k}{4\pi D_r} E_1 \left( 1, \frac{\vec{r}^2}{4D_r t} \right) \right], \quad (9)$$

where we have set  $t_0 = 0$  and used the definition of the exponential integral [63],  $E_1(a) = \int_a^\infty \exp(-t/t) dt$ .

Similar to the feeding behavior of *Daphnia*, the agent must forage in a bounded food patch for a fixed time. We consider the food patch to be a circle of radius,  $R$ , with no food outside the circle. Inside the circle the food is uniformly distributed, so that  $c(\vec{r}, t) = c_0$  for  $|\vec{r}| < R$ , and vanishing elsewhere, where the origin is at the center of the circle. Then, after a fixed time  $T$ , we calculate the food remaining in the patch,

$$C(T) = 2\pi c_0 \int_0^R \exp \left[ -\frac{k}{4\pi D_r} E_1 \left( \frac{r^2}{4D_r T} \right) \right] r dr. \quad (10)$$

First, let us analyze the parameters upon which  $C(T)$  is dependent. The ratio,  $\tilde{D} = \frac{R^2}{4T}$  has the dimension (*length*<sup>2</sup>/*time*) and thus is a characteristic diffusion constant. Note that the clearance rate,  $k$ , defined by Eq. (7) also has the dimension of a diffusion constant. Thus we can define two dimensionless parameters,  $\kappa = k/\tilde{D}$  and  $\delta = D_r/\tilde{D}$ , that govern the process. The first,  $\kappa$ , is the dimensionless clearance rate, and the second,  $\delta$ , is the dimensionless diffusion constant.

Changing the variable of integration to  $\xi = r^2/4D_r t$ , we obtain from Eq. (10), the following expression for the food remaining in the patch after time  $T$ ,

$$C(T) = C(0)\delta \int_0^{1/\delta} \exp \left[ -\frac{\kappa}{\delta} E_1(\xi) \right] d\xi, \quad (11)$$

where  $C(0) = 4\pi R^2 c_0$  is the initial amount of food in the patch. The fraction of food remaining after time  $T$  is

$$\frac{C(T)}{C(0)} = c_{\text{remaining}}(\kappa, \delta) = \delta \int_0^{1/\delta} \exp \left[ -\frac{\kappa}{\delta} E_1(\xi) \right] d\xi. \quad (12)$$

In order to obtain quantitative results, this expression can be evaluated numerically with the help of the expressions, Eqs. (5.1.53) and (5.1.54) in Ref. [63]. Instead of the fraction of food remaining in the patch, we could evaluate the fraction of food gathered by the agent,  $c_{\text{gathered}} = 1 - c_{\text{remaining}}$ . The results are shown in Fig. 8 where we plot the fraction of food gathered versus the dimensionless diffusion constant,  $\delta$ .

Fig. 8 shows that there exists a maximum of gathered food at a particular value of the dimensionless diffusion constant,  $\delta = D_r/\tilde{D}$ . Since  $D_r$  depends strongly and monotonously on the width of the exponential TAD, as shown in Eqs. (1) and (4), it is clear that there is an optimal width  $\sigma_0$  for which the food gathered is maximized corresponding to maximal foraging success. Thus our simple theory of food gathering is consistent with the hypothesis put forth at the beginning of this paper.

## 6. Random walk simulations

The foregoing simple theory indicates that exponential TADs with characteristic noise widths,  $\sigma_0$ , maximize food gathering in a finite sized food patch while feeding for a finite amount of time.

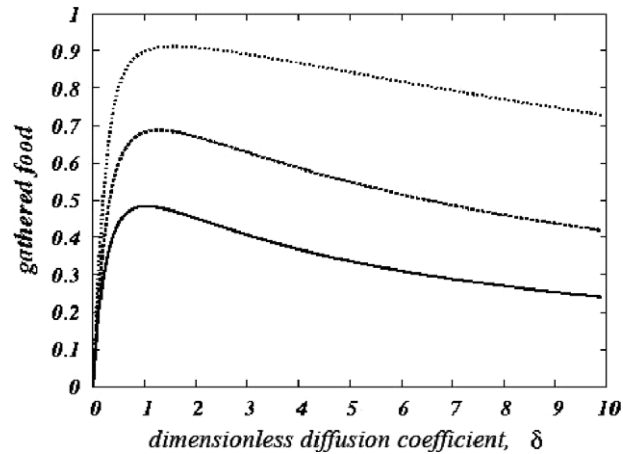


Fig. 8. Fraction of food gathered  $c_{\text{gathered}}$ , versus the dimensionless diffusion constant  $\delta$ , for three values of the dimensionless clearance rate  $\kappa = 1$  (solid line),  $\kappa = 2$  (dashed line),  $\kappa = 5$  (dotted line). Note the maximum of food gathered at an optimal value of  $\delta$ . The gathered food is expressed as a fraction of the total original amount.

We have tested this conclusion also with a numerical simulation. *Daphnia* do feed for a finite time (only at night) and we assume that the food patches are finite in size. There is now information on the measured sizes of such food patches in the range of decimeters [64]. Here we present two simulations built upon minimal sets of assumptions. Both indeed show a maximum in the food gathered at an optimal value of the TAD width.

### 6.1. First simulation

In this simulation the food gathered is proportional to total length traversed within the circular food patch, excluding path recrossing events where the food has already been consumed. The agent is assumed to eat only during a hop. Pauses and the pause times are ignored. The agent simply executes the CRW within the continuous space delineated by the circle. In this simulation a circle of radius  $R = 90$  mm is defined as a food patch. The circle is initially filled with  $2.5 \times 10^6$  boxes. The food density as represented by the boxes is uniform, and the agent hops always with the same hop length equal to the measured mean length as quoted in Section 4,  $\langle \ell \rangle = 1.11$  mm. Thus an agent encounters on average 100 food boxes (prey particles) during one hop. Ten agents are initially located at random positions within the circle. The system is iterated for a finite number of times (representing the finite feeding time,  $T$ ). Upon each iteration each agent (1) chooses a turning angle,  $\alpha$ , from an exponential distribution of width  $\sigma_0$ ; and (2) hops for a fixed and constant length in the direction dictated by  $\alpha$ . The numbers of left-hand and right-hand turns are equal in the mean. During the hop, all boxes that the agent encounters (i.e. that its trajectory overlaps with) are marked. Outside the circle the agent obtains nothing. It should be noted that an agent that has exited the patch can (with small probability) actually return to the circle within which it again collects food if it encounters boxes not previously marked. After the  $n$  iterations, the marked boxes within the circle are summed and expressed as a percentage of the total initial number of boxes within the circle. This represents the ‘food gathered’ by all agents during the

finite foraging time. The system is reinitialized and the process repeated until a statistically accurate average value for the food gathered is obtained. This is the output of the simulation: the mean food gathered in the specified time within the specific sized food patch. The fixed foraging time is  $T = n\tau$ , where  $\tau$  is the total interhop time. This simulation is repeated for various noise widths spanning the range of distributions from close to a delta function to close to pure Brownian motion. The results are shown in Fig. 9.

In Fig. 9, the collected material is the food gathered expressed as a fraction of the total initial food placed in the circle. The simulation shows a maximum in the amount of material gathered at an optimal value of noise width. In this simulation the values of  $R$  and  $T$  were chosen to locate the maximum at approximately  $\sigma_0 = 1.0$  radian ( $57.3^\circ$ ). This corresponds to the observed value of the noise width for *D. magna* – juveniles (see Table 1).

Alternatively, the simulation can be used to calculate the optimal food patch radius given a fixed noise width and feeding time. For a single agent started at the center of the patch, and for  $T = n\tau = 60$  s,  $\sigma_0 = 1.20$  rad (see *D. magna* – adult, in Table 1) and  $\tau = \langle t_h \rangle + \langle t_p \rangle = 0.4$  s, we obtain  $R_{\text{opt}} = 36$  mm.

While the results of this simulation are not unreasonable, one might ask how far the typical agent diffuses in the fixed feeding time? We can estimate the diffusion distance based purely on experimentally measured values, for example, for *D. magna* – adult: the mean hop length,  $\langle \ell \rangle = 1.11$  mm; hop time,  $\langle t_h \rangle = 0.15$  s; pause time,  $\langle t_p \rangle = 0.25$  s, and optimal turning angle  $\sigma_0 = 1.2$  rad, as follows. From the theory Eq. (4), the normalized correlation is

$$\Omega = \frac{1 + \exp(-\pi/\sigma_0)}{1 - \exp(-\pi/\sigma_0)} \frac{\sigma_0^{-2}}{1 + \sigma_0^{-2}} \cong 0.47 \quad (5.1)$$

and the diffusion constant, Eq. (1) is

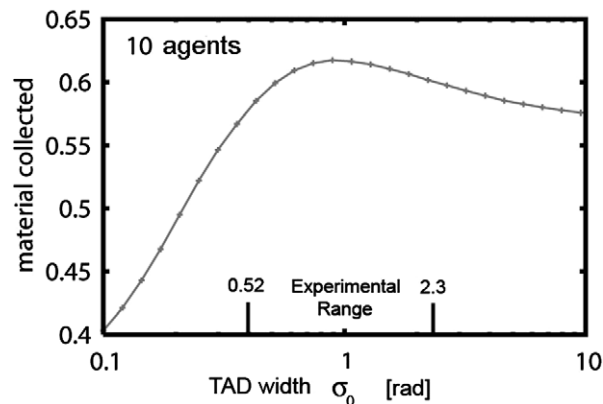


Fig. 9. The first simulation. Ten agents were initially located at random positions within a circle of radius  $R = 90$  mm. They forage for food (material) with a sequence of hops of length 1 mm and hop time 0.4 s for a fixed time  $T = 60$  s. Turning angles are chosen from exponential distributions of noise widths  $\sigma_0$ . The experimentally measured range for all species is shown by the vertical bars on the bottom axis. At each  $\sigma_0$ , 50000 realizations of the population were executed. The statistical precision is comparable to the size of the symbols, as indicated by the smoothness of the curve.

$$D_r \cong \frac{\langle \ell^2 \rangle}{4\tau} \frac{1 + \Omega}{1 - \Omega} \cong 2.17 \text{ mm}^2/\text{s}, \quad (5.2)$$

with the interhop time,  $\tau = 0.4$  s. This diffusion constant is in surprisingly good agreement with that calculated from theory alone using reasonable assumptions [12]. Thus in a foraging time of 60 s in two dimensions the typical animal would diffuse a distance of  $R_{\text{rms-diffusion}} = \sqrt{4DT} \cong 22.8$  mm. In a total feeding time of 8 h the agent would diffuse about 0.5 m. We note that  $R_{\text{rms-diffusion}} < R_{\text{opt}}$ , and this is to be expected. Recall that  $R_{\text{opt}}$  is the fixed food patch radius obtained by adjusting the maximum of food gathered to correspond to a particular value of  $\sigma_0$ . Considering the food missed, with fixed  $T$  and  $R$ , there are two possibilities: First, the agent may wander outside of the food patch, in which case it obtains nothing. Second, if the agent crosses its own or another agent's path inside the food patch, where the food is already eaten, it obtains nothing in the overlap of the two tracks. Thus the optimal radius marks an equilibrium of these two cases. Because the loss in the first case is larger than in the second, the diffusion radius is always smaller than the optimal radius.

## 6.2. The second simulation

The second simulation may represent a more realistic view of how *Daphnia* actually feed. In this simulation the agents do not collect food during a hop, but instead during the pause time. Again we take a food patch represented by a circle of radius  $R$ . The circle is filled with  $2.5 \times 10^6$  boxes initially as before. We assume a random walk-type motion consisting of the hop–pause–turn–hop sequence with fixed hop length  $\ell$ , fixed hop time  $t_h$  and pause time  $t_p$ . The hop length and time are taken from experimentally obtained average values (see Section 4),  $\langle \ell \rangle = 1.11$  mm; hop time,  $\langle t_h \rangle = 0.15$  s. The pause times are taken from a distribution with characteristic parameters as measured by experiment, that is with average  $\langle t_p \rangle = 0.25$  s. The pause times were thus chosen randomly from the pause time distribution:  $P(t_p) = \exp[-t/0.25]$ . The turning angles between hops are taken from an exponential distribution of width  $\sigma_0$  as given by Eq. (3). Right and left hand turns are randomly chosen and on average are equal in number (so that the TAD is symmetric). Initially, the agent is started from the center of the circle. After every hop, the agent stops (the pause time) to gather food. Depending on the pause time and the clearance rate  $k$ , chosen, a circle of a certain size is drawn around the  $x$ – $y$  position of the pause. All boxes fully or partially within this circle are removed (the food is eaten and no longer available to that or another agent). As before an agent may exit the circle where it finds no food and may re enter the circle (with some probability) and find food again. Sequential values of  $\sigma_0$  are chosen in the range 0.1–10 rad, and the simulation was run for each value. After a fixed time  $T = 120$  s (corresponding to 50000 iterations) the number of boxes removed (food eaten) is calculated as a percentage of the initial total number as before. This constituted one ‘run’ of the simulation. Another agent was then started in a random initial direction for the second run. This process was repeated for 5000 runs in order to obtain a statistically precise mean value for the food gathered at every value of  $\sigma_0$ . This sequence was repeated for three values of the clearance rate  $k$ . The results are shown in Fig. 10 where we again delineate the experimentally observed range (ER).

We are gratified that the main result of both simulations is robust, that is, two quite different simulations both show the optimal TAD width that maximizes the food gathered, and this is our main result.

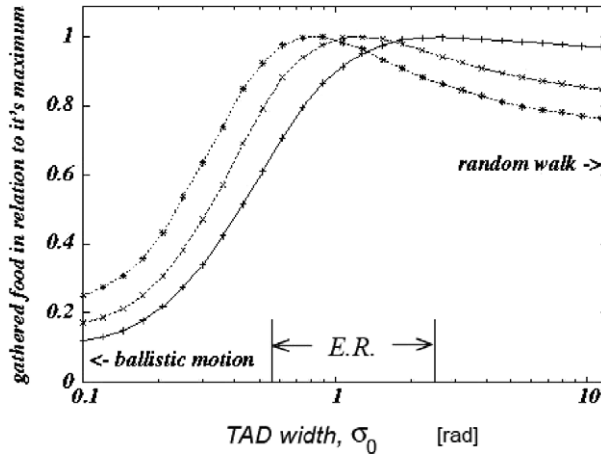


Fig. 10. The gathered food versus the width of the TAD  $\sigma_0$ , for three clearance rates:  $k = 32 \text{ mm}^2/\text{s}$  (solid curve),  $8 \text{ mm}^2/\text{s}$  (dashed curve), and  $2 \text{ mm}^2/\text{s}$  (dotted curve). These test the sensitivity of the simulation to parameter values. The statistical precision is comparable to the size of the symbols. Here the gathered food in each case has been normalized so that its maximum is unity. ER delineates the experimentally observed range.

Three typical trajectories for three values of  $\sigma_0$  are shown in Fig. 11 for this simulation. One can clearly see that for  $\sigma_0$  too large (magenta), the agent spends too much time near the origin and too little exploring the outer regions of the food patch, while for  $\sigma_0$  too small (blue) the trajectory is nearly ballistic and again too little food is obtained. The optimal noise width (green) yields the maximum coverage and hence the maximum food obtained.

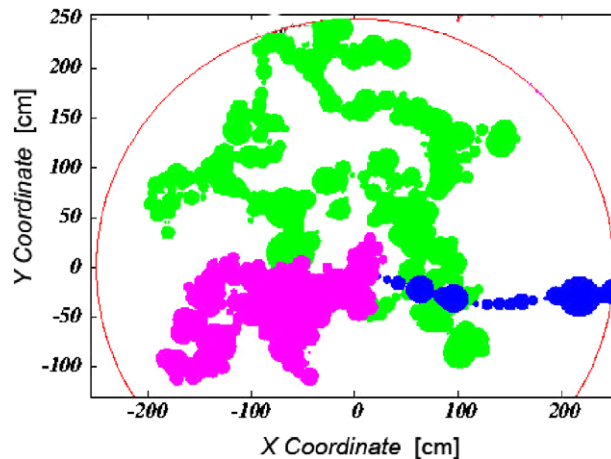


Fig. 11. Sample trajectories showing food consumed during each pause as the size of each circle at every  $x$ - $y$  location during a pause separating two successive hops. The blue trajectory represents nearly ballistic motion for  $\sigma_0 = 0.1$ . The green trajectory is for  $\sigma_0 = 1.2$  and is optimal for this simulation. The magenta trajectory is for  $\sigma_0 = 10.0$  and represents nearly uncorrelated, or pure Brownian, motion. (For interpretation of the references to color in this figure legend, the reader is referred to the web version of this paper.)

## 7. Speculation, testing and conclusions

Our hypothesis is that the exponential TADs including a specific range of noise widths represent a foraging characteristic that has evolved in order to enhance survival. The experimental data together with the theory and the simulations based on minimal assumptions support, though do not prove, the hypothesis. However, both the theory and the simulations show that an optimal noise width leads to a maximum of food gathered in a finite feeding time in a finite sized food patch provided the TAD is an exponential function. In the experiment, we observe that four of the five species including juveniles of two species of *Daphnia* do show TADs that are well described by exponential functions. We can therefore conclude that the exponential TADs observed for the animals lead to an optimal foraging behavior in the form of a maximum in the food gathered at an optimal value of noise width of the TAD. Moreover, commencing with experimental values for the mean hop length, hop and pause times, using our theory and simulations, we obtain reasonable numbers for the patch size based on typical short or night-long feeding times.

## 8. Discussion

This work does not, of course, prove the conjecture. In fact, we make the following criticisms of our work: First, the range of noise widths  $\sigma_0$ , is rather wide, from 0.52 rad (*D. pulex* juvenile) to 2.3 rad (*D. lumholtzi* with spines) as shown in Table 1. This observation argues against our interpretation of the noise width as *universally* leading to optimal foraging success. On the other hand, if the two extreme values just mentioned are eliminated, all other values of  $\sigma_0$  lie in the rather more narrow range between 0.74 rad (*D. pulex* adult) and 1.2 rad (*D. magna* adult). The interpretation – that maximum foraging success leads to maximum fitness – would strictly point toward a *single* (optimal) value of  $\sigma_0$  for all species, ages and morphological forms. But the detailed complexity of each individual organism no doubt precludes such universality. A second criticism addresses the reproducibility of results obtained in the two different labs in St. Louis and Milwaukee. As stated above, we have two sets of data for *D. pulex* adult, one obtained in St. Louis and the other in Milwaukee representing an 11% difference. This difference can be considered to represent the overall reliability of our results. (One might note, however, that the St. Louis result as shown in Fig. 6 is one of the very few histograms that show a ‘cross over’ behavior from exponential to possibly power law behavior. Thus the formal fit to the data over the full range of turning angle may have been skewed toward a smaller than normal value. Similar cross over, or main discontinuities, were observed in histograms of tumbling angles by *Oxyrrhis marina* in Ref. [69]). Finally, it should be noted that our simulations and experiments differ in one important respect: In the simulations, the agent can leave the food patch and even return to it with some probability. By contrast, in the experiments the animal always swims in a food patch of uniform and constant food distribution. The experimental results thus represent a natural behavior of single individuals while foraging within a food patch of sufficient prey density. We assume that the characteristics of this motion, for example the noise width, evolved over time and under natural conditions, for example, within finite sized food patches and during finite feeding times encountered in the wild.

It is important to note that we have not produced a comprehensive theory of motion in this work. Instead, our message is quite simple: Based on experimental observations, histograms of

the turning angles of foraging *Daphnia* are well described by exponential functions of varying widths. Under the constraint that the agents feed for a fixed time in a food patch of fixed size, theory and simulation show that the food gathered is maximized at an optimal value of the width of the TAD. The influences of gravity and fluid drag on feeding [65,66] are not considered here.

Exponential distributions are not common in physics but have recently begun to attract attention in biology, for example in descriptions of the swimming velocities of diverse types of motile cells [67]. Quoting these authors [67] “. . . in spite of the complex cellular processes, the motion of a cell can be well described by a simple universal distribution function.” Distributions of the rate of turning angles have recently been reported, and the distributions of path curvature for the planktonic organism, *O. marina*, both with and without the presence of prey, appear to be describable by exponentials [68]. Using the same organism, Bartumeus et al. [69] assembled histograms of tumbling angles and studied the searching statistics of these animals under the influence of varying density of prey. They found evidence of exponential flight time distributions when prey are plentiful, switching over to a power law (possibly Lévy) statistics when prey become scarce. Moreover, one previous measurement of the TAD for a marine planktonic organism, *Temora longicornis* has been reported [32]. Mean turning angles [17,18,34–36,38] and turning angle distributions [29,37,43–45,69] for a variety of animals and theoretical models have been reported previously. The use of mean turning angles specifically in search strategies have been reported for copepod foraging using a special simulator [17], clown fish larvae [18], the painted turtle [35] and in general motion problems for the fruit fly [34] and cultured trout fish [36]. The mean turning angle also arises in theoretical analyses of biased CRWs [38]. For biased CRWs, the TAD cannot be symmetrical as in Fig. 5 here, since in these cases the animal is turning in response to some stimulus. Thus the mean turning angle becomes time dependent. Turning angle distributions were reported in the following cases: A general model for animal motion in a bounded space also results in asymmetric TADs generated as the animal turns to avoid the boundaries [29]. Asymmetric TADs must also be integrated in models applied to motions of desert arthropods [37]. Foraging bumblebees also show TADs specifically when their habitat is heterogeneous on scales smaller than the mean range [43]. Finally, two theoretical models make use of TADs, one an involving chaos and fractal motions in a fish school [44]; and the other a general model of animal motion using persistent, or biased, CRWs [45]. Interestingly, correlations using TADs between the turning angles and other motionally relevant quantities were studied [39]. TADs are crucial in the analysis of animals displaying non-Brownian motions, for example Lévy statistics [69]. Of these studies, three [17,29,35] specifically address the problem of animal motions in bounded spaces as we do here. None, however, apply both constraints: bounded space and fixed time to the motion as we do here. None have found an optimum search strategy mediated by noise as we do here. In contrast to swarming behavior [70], which may be a predator avoidance strategy [71], all of the previously cited works, and the present study, apply to individual motions (as contrasted with collective motions) in response to single stimuli insofar as possible.

Regarding search strategies, a strong influence seems to be the ‘patchiness’ or heterogeneity of the prey distribution [23]. Generally, search strategies that call upon Lévy statistics are more efficient than purely Brownian statistics when the prey distribution is highly heterogeneous [1,2,69]. By contrast here we study only uniform prey distributions of high concentration but with foraging limited by two aforementioned constraints in the theory and simulations.

Fig. 9, which shows maximum foraging success at an optimal noise width,  $\sigma_0$ , is reminiscent of stochastic resonance (SR) [72]. The defining signature of SR is that some useful quantity, for example, information about the approach of predators [73,74] or the presence of prey [75] is optimized by noise. The noise can be either provided by external or endogenous sources. Since noise has always been present, it is, of course, an attractive idea that noise, whether endogenous or environmental, in some way mediated or partially mediated the evolution of many sensory and functional modalities that we see in nature today, and that internal random appearing processes, like the observed TADs, may have arisen in response to selective pressures. The obvious difficulty to test this supposition is that it is impossible to change the evolved characteristic (in this case, the noise width) in a controlled manner in an experimental animal in the lab. (In the case of *Daphnia* it is possible to change this width in the lab by applying another stimulus, for example light. But in that case we would not be observing natural foraging behavior alone under the influence of uniform food density in the dark as occurs in nature.) Indeed, nearly all laboratory stochastic resonance experiments to date, both in physics and biology, have been performed with external noise intensity as a variable under the control of the experimenter. (Exceptions are two experiments in medical science wherein an internal neural noise was controlled by muscle tension [76,77]). One experiment, similar in spirit to the present one, found that a characteristic internal noise intensity closely matched measured optimal values obtained in a controlled experiment, thus admitting an interpretation based on natural selection [78]. Much has been written about SR, and here we cite the progress report [72] and the reviews (in chronological order) [79–82].

Our approach has consequently been to obtain measurements of the hypothetically evolved quantity (in this case the TADs and their widths) across species representing differing sizes and swimming characteristics. The idea being that if the quantity has indeed arisen because of natural selection in order to maximize success at a common task (in this case, foraging for food) then it may have appeared across species and be similar for differing species. Here we have shown that exponential TADs are observed for four species including two morphological forms of one and for both adults and juveniles of two other species. Moreover, we have shown that the characteristic noise widths of all these TADs lie in a quite reasonable though rather wide range that our simulation shows to be near optimal. Though our results are suggestive, we cannot unequivocally say that our *Daphnia* demonstrate a naturally evolved example of SR. However, the theory and simulations presented above, specifically the results shown in Figs. 8–10, point toward this suggestion and thus demonstrate a new kind of SR that we call, *natural stochastic resonance*.

## Acknowledgements

We thank Werner Ebeling, of Humboldt University in Berlin and Michael Hofmann of Center for Neurodynamics, in St. Louis for stimulating discussions. We are grateful to Jennifer Forecki of the Great Lakes WATER Institute in Milwaukee for making the cell density measurements. FM is grateful to the Alexander von Humboldt Foundation for continuing support. JRS acknowledges support by the National Science Foundation, grant OCE-0352264. LSG, UE and SG acknowledge support from the German Science Foundation, SFB 555.

## References

- [1] G.M. Viswanathan, S.V. Buldyrev, S. Havlin, M.G.E. Da Luz, E.P. Raposo, H.E. Stanley, Optimizing the success of random searches, *Nature* 401 (1999) 911.
- [2] F. Bartumeus, J. Catalan, U.L. Fulco, M.L. Lyra, G.M. Viswanathan, Optimizing the encounter rate in biological interactions: Lévy versus Brownian strategies, *Phys. Rev. Lett.* 88 (2002), 097901 and 89 (2002) 109902.
- [3] H.C. Berg, *Random Walks in Biology*, Princeton University, Princeton, New Jersey, 1993.
- [4] A. Okubo, S.A. Levin (Eds.), *Diffusion and Ecological Problems: Modern Perspectives*, second ed., Springer, New York, 2001.
- [5] D. Wolpert, W. MacReady, No Free Lunch Theorems for Optimization, *IEEE Trans. Evol. Comput.* 1 (1997) 67.
- [6] A.Y. Keiyu, H. Yamazaki, J.R. Strickler, A new modelling approach for zooplankton behaviour, *Deep-Sea Res. II* 41 (1994) 171.
- [7] A. Okubo, D. Grünbaum, *Mathematical Treatment of Biological Diffusion* in Ref. [4], Chapter 5, pp. 127–162.
- [8] D. Grünbaum, Advection-diffusion equations for generalized tactic searching behaviors, *J. Math. Biol.* 38 (1999) 169.
- [9] A.W. Visser, U.H. Thygesen, Random motility of plankton: diffusive and aggregative contributions, *J. Plankton Res.* 25 (2003) 1157.
- [10] A.H. Øien, Daphnic dynamics based on kinetic theory: an analogue-modelling of swarming and behaviour of *Daphnia*, *Bull. Math. Biol.* 66 (2004) 1.
- [11] M. Uttieri, M.G. Mazzochi, Ai Nihongi, M.R. D'Alcalà, J.R. Strickler, E. Zambianchi, Discussion of relative strengths of noise and deterministic components of motion. Suggestion that noise evolved as a predator avoidance measure, *J. Plankton Res.* 26 (2004) 99.
- [12] L. Schimansky-Geier, U. Erdmann, N. Komin, Advantages of hopping on a zig-zag course, *Phys. A* 351 (2005) 51.
- [13] D. Grünbaum, Advection-diffusion equations for internal state-mediated random walks, *SIAM J. Appl. Math.* 61 (2000) 43.
- [14] K.M. Cuddington, E. McCauley, Food-dependent aggregation and mobility of the water fleas *Ceriodaphnia dubia* and *Daphnia pulex*, *Can. J. Zool.* 72 (1994) 1217.
- [15] P.H. Lenz, J.E. Hartline, J.E. Purcell, D.L. Macmillan (Eds.), *Zooplankton: Sensory Ecology and Physiology*, Gordon and Breach Publishers, Amsterdam, 1996.
- [16] P. Larsson, O.T. Kleiven, Food Search and Swimming Speed in *Daphnia* in Ref. [15], pp. 375–388.
- [17] A.W. Leising, Copepod foraging in thin layers using SEARCH (Simulator for Exploring Area-Restricted search in Complex Habitats) 2 (2002) 1–18.
- [18] D.J. Coughlin, J.R. Strickler, B. Sanderson, Swimming and search behaviour in clownfish, *Amphiprion perideraion*, larvae, *Anim. Behav.* 44 (1992) 427.
- [19] J. Yen, B.G. Sanderson, J.R. Strickler, A. Okubo, Feeding currents and energy dissipation by *Euchaeta rimana*, a subtropical pelagic copepod, *3 Limnol. Oceanography* 6 (1991) 362.
- [20] A.W. Visser, T. Kjørboe, Plankton motility patterns and encounter rates, *Oecologia* 148 (3) (2006) 538.
- [21] J.D. Wiggert, A.G.E. Haskell, G.-A. Paffenhöfer, E.E. Hofmann, J.M. Klinck, The role of feeding behavior in sustaining copepod populations in the tropical ocean, *J. Plankton Res.* 27 (10) (2005) 1013.
- [22] M. Mazzocchi, G. Paffenhöfer, Swimming and feeding behaviour of the planktonic copepod *Clausocalanus furcatus*, *J. Plankton Res.* 21 (1999) 1501.
- [23] S.A. Levin, L.A. Segel, Hypothesis for origin of planktonic patchiness, *Nature* 259 (1976) 659.
- [24] S.A. Levin, Patchiness in marine and terrestrial systems: from individuals to populations, *Phil. Trans. Roy. Soc. Lond. B* 343 (1994) 99.
- [25] A. Okubo, J.G. Mitchell, Patchy Distribution and Diffusion, in Ref. [4], Chapter 9, pp. 268–294.
- [26] D. Grünbaum, Using spatially-explicit models to characterize foraging performance in heterogeneous landscapes, *Am. Natur.* 151 (2) (1998) 97.
- [27] P.J.S. Franks, L.J. Walstad, Phytoplankton patches at fronts: a model of formation and response to wind events, *J. Marine Res.* 55 (1997) 1.
- [28] P.J.S. Franks, J.S. Jaffe, Microscale distributions of phytoplankton: initial results from a two-dimensional imaging fluorometer, *OSST. Mar. Eco. Prog. Ser.* 220 (2001) 59.

- [29] R. Jeanson, S. Blanco, R. Fournier, J.-L. Deneubourg, V. Fourcassié, G. Theraulaz, A model of animal movements in a bounded space, *J. Theor. Biol.* 225 (2003) 443.
- [30] S.I. Dodson, Optimal Swimming Behavior of Zooplankton, in Ref. [15], pp. 365–374.
- [31] G.A. Parker, J. Maynard Smith, Optimality theory in evolutionary biology, *Nature* 348 (1990) 27.
- [32] F.G. Schmitt, L. Seuront, Multifractal random walk in copepod behavior, *Phys. A* 301 (2001) 375.
- [33] M. Uttieri, E. Zambianchi, J.R. Strickler, M.G. Mazzochi, Fractal characterization of three-dimensional zooplankton swimming trajectories, *Eco. Model.* 185 (2005) 51.
- [34] J.-R. Martin, A portrait of locomotor behaviour in *Drosophila* determined by a video-tracking paradigm, *Behav. Proc.* 67 (2004) 207.
- [35] David R. Bowne, Heather R. White, Searching strategy of the painted turtle *Chrysemys picta* across spatial scales, *Anim. Behav.* 68 (2004) 1401.
- [36] M.-L. Bégout Anras, J.P. Lagardère, Measuring cultured fish swimming behaviour: first results on rainbow trout using acoustic telemetry in tanks, *Aquaculture* 240 (2004) 175.
- [37] T. Merkle, M. Rost, W. Alt, Egocentric path integration models and their application to desert arthropods, *J. Theor. Biol.* 240 (2006) 385.
- [38] E.A. Codling, N.A. Hill, Sampling rate effects on measurements of correlated and biased random walks, *J. Theor. Biol.* 233 (2005) 573.
- [39] M. Wiktorsson, T. Rydén, E. Nilsson, G. Bengtsson, Modelling the movement of a soil insect, *J. Theor. Biol.* 231 (2004) 497.
- [40] P. Turchin, Quantitative Analysis of Movement: Measuring and Modelling Population Redistribution in Animal and Plants, Sinauer Associates Inc., Sunderland, MA, 1998.
- [41] P.M. Kareiva, N. Shigesada, Analyzing insect movement as a correlated random walk, *Oecologia* 56 (1983) 234.
- [42] P.A. Zollner, S.L. Lima, Search strategies for landscape-level interpatch movements, *Ecology* 80 (1999) 1019.
- [43] M. Goverde, K. Schweizer, B. Baur, A. Erhardt, Small-scale habitat fragmentation effects on pollinator behaviour: experimental evidence from the bumblebee *Bombus veteranus* on calcareous grasslands, *Biol. Conserv.* 104 (2002) 293.
- [44] D.A. Tikhonov, H. Malchow, Chaos and fractals in fish school, motion, II, *Chaos, Solit. Fract.* 16 (2003) 287.
- [45] H.-i. Wu, B.-L. Li, T.A. Springer, W.H. Neill, Modelling animal movement as a persistent random walk in two dimensions: expected magnitude of net displacement, *Ecol. Model.* 132 (2000) 115.
- [46] M. Uttieri, M.G. Mazzochi, Ai Nihongi, M.R. D'Alcalá, J.R. Strickler, E. Zambianchi, Lagrangian description of zooplankton swimming trajectories, *J. Plankton Res.* 26 (2004) 99.
- [47] W.C. Lemon, Fitness consequences of foraging behaviour in the zebra finch, *Nature* 352 (1991) 153.
- [48] A. Houston, C. Clark, J. McNamara, M. Mangel, Dynamic models in behavioural and evolutionary ecology, *Nature* 332 (1988) 29.
- [49] N. Komin, U. Erdmann, L. Schimansky-Geier, Random walk theory applied to *Daphnia* motion, *Fluct. Noise Lett.* 4 (2004) L151.
- [50] T.M. Zaret, J.S. Suffern, Vertical migration in zooplankton as a predator avoidance mechanism, *Limnol. Oceanogr.* 21 (1976) 804.
- [51] J. Ringelberg (Ed.), Diel Vertical Migration of Zooplankton, *Arch. F. Hydrobiol. – Adv. Limnol.* 39 (1993) 1–222.
- [52] W. Lampert, Ultimate causes of diel vertical migration of zooplankton: new evidence for the predator-avoidance hypothesis, *Arch. Hydrobiol. Beih.* 39 (1993) 79.
- [53] S.M. Bollens, D.W. Frost, Predator induced diel vertical migration in a planktonic copepod, *J. Plankton Res.* 11 (1989) 1047.
- [54] E. van Gool, J. Ringelberg, Light-induced migration behaviour of *Daphnia* modified by food and predator kairomones, *Anim. Behav.* 56 (1998) 741.
- [55] S.C. Rhode, M. Pawlowski, R. Tollrian, The impact of ultraviolet radiation on the vertical distribution of zooplankton of the genus *Daphnia*, *Nature* 412 (2001) 69.
- [56] A. Ordemann, G. Balazsi, F. Moss, Motions of *Daphnia* in a light field: random walks with a zooplankton, *Nova Acta Leopoldina NF* 88, Nr. 332 (2003) 87–103 (Proc. German Academy of Science).
- [57] A. Ordemann, G. Balazsi, F. Moss, Pattern formation and stochastic motion of the zooplankton *Daphnia* in a light field, *Phys. A* 325 (2003) 260.

- [58] N. Shigesada, K. Kawasaki, *Biological Invasions: Theory and Practice*, Oxford University, Oxford, 1977.
- [59] P.M. Kareiva, N. Shigesada, Analyzing insect movement as a correlated random walk, *Oecologia* 56 (1983) 234.
- [60] J.A. Byers, Correlated random walk equations of animal dispersal resolved by simulation, *Ecology* 82 (2001) 1680.
- [61] A. Okubo, P. Kareiva, Some Examples of Animal Diffusion, in Ref. [4], Chapter 6, pp. 170–196.
- [62] A. Okubo, Horizontal dispersion and critical scales for phytoplankton patches, in: J.H. Steele (Ed.), *Spatial Patterns in Plankton Communities*, Plenum, New York, 1978.
- [63] M. Abramowitz, I.A. Stegun, *Pocketbook of Mathematical Functions*, Harri Deutsch, Frankfurt a Main, 1984. (Chapter 5).
- [64] P.J.S. Franks, J.S. Jaffe, Microscale distributions of phytoplankton: initial results from a two-dimensional imaging fluorometer, *OSST. Mar. Eco. Prog. Ser.* 220 (2001) 59.
- [65] J.R. Strickler, Gravity, drag and feeding currents of small zooplankton, *Science* 228 (1985) 1017.
- [66] J. Gerritsen, K.G. Porter, J.R. Strickler, Not by sieving alone: suspension feeding in *Daphnia*, *Bull. Mar. Sci.* 43 (1988) 366.
- [67] A. Czirók, K. Schlett, E. Madarász, T. Vicsek, Exponential distribution of locomotion activity in cell cultures, *Phys. Rev. Lett.* 81 (1998) 0031.
- [68] S. Menden-Deuer, D. Gruenbaum, Individual foraging behaviors and population distributions of a planktonic predator aggregating to phytoplankton thin layers, *Limnol. Oceanogr.* 51 (2006) 109.
- [69] F. Bartumeus, F. Peters, S. Pueyo, C. Marrasé, J. Catalan, Helical Lévy walks: adjusting searching statistics to resource availability in microzooplankton, *PNAS* 100 (2003) 12771.
- [70] J. Vollmer, A. Gergely Vegh, C. Lange, B. Eckhardt, Vortex formation by active agents as a model for *Daphnia* swarming, *Phys. Rev. E* 73 (2006) 061924.
- [71] M. Milanski, Do all members of a swarm suffer the same predation? *Z. Tierpsychol.* 45 (1977) 373.
- [72] K. Wiesenfeld, F. Moss, Stochastic resonance: from Ice Ages to Crayfish and Squids, *Nature* 373 (1995) 33.
- [73] J. Douglass, L.A. Wilkens, E. Pantazelou, F. Moss, Noise enhancement of information transfer in crayfish mechanoreceptors by stochastic resonance, *Nature* 365 (1993) 337.
- [74] J. Levin, J. Miller, Broadband neural encoding in the cricket cercal sensory system by stochastic resonance, *Nature* 380 (1996) 165.
- [75] D. Russell, L. Wilkens, F. Moss, Use of behavioral stochastic resonance by paddlefish for feeding, *Nature* 402 (1999) 219.
- [76] F.Y. Chiou-Tan, K.N. Magee, L.R. Robinson, M.R. Nelson, S.M. Tuel, T.A. Krouskop, Enhancement of subthreshold sensory nerve action potentials during muscle tension mediated noise, *Intern. J. Bifurc. Chaos* 6 (1996) 1389.
- [77] P. Cordo, J. Inglis, S. Verschueren, J.J. Collins, D. Merfeld, S. Rosenblum, S. Buckley, F. Moss, Noise in human muscle spindles, *Nature* 383 (1996) 769.
- [78] F. Jaramillo, K. Wiesenfeld, Mechano-electrical transduction assisted by Brownian motion: a role for noise in the auditory system, *Nat. Neurosci.* 1 (1998) 384.
- [79] D. Pierson, D. O’Gorman, F. Moss, Stochastic resonance: tutorial and update, invited review, *Int. J. Bifurcat. Chaos* 4 (1995) 1.
- [80] L. Gammaitoni, P. Hanggi, P. Jung, F. Marchesoni, Stochastic Resonance, *Rev. Mod. Phys.* 70 (1998) 223.
- [81] V. Anishchenko, F. Moss, A. Neiman, L. Shimansky-Geier, Stochastic resonance: noise induced order, *Sov. Phys. Usp.* 42 (1) (1999) 7.
- [82] F. Moss, L.M. Ward, W.G. Sannita, Stochastic resonance and sensory information processing: a tutorial and review of application, *Clin. Neurophysiol.* 115/2 (2004) 267.